International Journal of Fatigue 31 (2009) 1742–1750

Contents lists available at ScienceDirect

International Journal of Fatigue

journal homepage: www.elsevier.com/locate/ijfatigue

Mean stress relaxation during cyclic straining of high strength aluminum alloys

Attilio Arcari [b], Raffaella De Vita [b], Norman E. Dowling [a,*]

[a] Materials Science and Engineering Department, and Engineering Science and Mechanics Department (Jointly Appointed), Virginia Polytechnic Institute and State University, Blacksburg, VA 24061, USA
[b] Engineering Science and Mechanics Department, Virginia Polytechnic Institute and State University, Blacksburg, VA 24061, USA

ARTICLE INFO

Article history:
Received 10 September 2008
Received in revised form 27 January 2009
Accepted 29 January 2009
Available online 5 February 2009

Keywords:
Aluminum alloys
Cyclic stress relaxation
Mathematical modeling
Mean stress

ABSTRACT

Cycle-dependent relaxation may alter mean stress values and thus affect fatigue crack initiation life. This phenomenon is an issue both for accuracy of estimated fatigue lives and for the success of methods of intentionally introducing beneficial mean stresses. Although rigorous plasticity theories may describe cycle-dependent relaxation, it is not feasible to incorporate their complex mathematics into strain-based life estimates when loading histories contain millions of cycles. Empirical models are, on the other hand, more numerically efficient and, therefore, for the present purpose, constitute a better choice for modeling this transient phenomenon. Experiments have been performed to study mean stress relaxation in aluminum alloys 7075-T6511 and 7249-T76511. Preliminary tests were also conducted on alloy 7475-T651. Two empirical models are used to illustrate the experimentally observed cycle-dependent relaxation.

1. Introduction

Mean stress can significantly increase or decrease the life for crack initiation in fatigue loading of engineering materials and mechanical components. At stress raisers, the local mean stress strongly influences the life to crack initiation. A number of different models have been developed for including mean stress effects in fatigue life calculations, such as those of Goodman, of Morrow, and of Smith–Watson–Topper (SWT) [1]. For aluminum alloys, the SWT method gives reasonably accurate results and so is a good choice [2]. A common practice in engineering design is to introduce compressive surface residual stresses, as these act as local mean stresses, having the beneficial effect of retarding fatigue crack initiation and early growth.

Both tensile and compressive mean stresses are subject to cyclic relaxation under biased deformation, as shown in Fig. 1 for a tensile case. Cyclic mean stress relaxation can affect fatigue life by causing loss of beneficial surface residual stress. Although cyclic stress relaxation has been the subject of a number of investigations there is still a need for improved empirical models capable of providing accurate predictions. Cyclic relaxation and other transient stress–strain phenomena are predicted by some comprehensive plasticity theories, but the mathematical formulations in these theories are generally too complex to allow efficient computation in the context of computer programs for strain-based fatigue life prediction [3–6], where it may be necessary to follow millions of variable amplitude cycles.

An early attempt to model cyclic mean stress relaxation for steel was reported by Morrow and Sinclair in 1958 [7]. Their theory was based on the concept that the amount of relaxation that occurs is dependent on the plastic deformation involved. The mean stress was expressed as a nonlinear function of cycle number, stress amplitude, the material's cyclic yield stress and strain, as well as its strain hardening exponent. Other methods and models have been developed to study the related problem of residual stress relaxation. (Residual stresses are internal stresses that are present even under zero applied loading, so that they alter the local mean stress and thus affect the fatigue life.) Beneficial compressive, near-surface residual stresses are introduced by various processes, such as shot peening, laser peening, low plasticity burnishing, and induction hardened [8].

In 1988, Landgraf and Chernenkoff [9] conducted a series of tests on axial specimens of steels, with the objective of evaluating the effect on fatigue life of mechanical or thermal processes employed to create residual stresses. They showed a dependence of mean stress relaxation on strain amplitude and material hardness, and they postulated the existence of a strain amplitude threshold below which no relaxation is exhibited.

In a study on cyclic relaxation of mean stresses in a nickel-based superalloy, Fang and Berkovits [10] found a transition between regions of strong and weak relaxation effects around 0.5% strain amplitude. This value is of the same order as the threshold levels in the Landgraf work. Stable values of mean stress at half of the fatigue life were recorded for various test conditions, and a relationship was found with strain amplitude. The variation of stable mean stress with strain amplitude was approximately linear up to the transition, and then followed a nonlinear relationship.

* Corresponding author.
E-mail address: ndowling@vt.edu (N.E. Dowling).

0142-1123/$ - see front matter © 2009 Elsevier Ltd. All rights reserved.
doi:10.1016/j.ijfatigue.2009.01.021

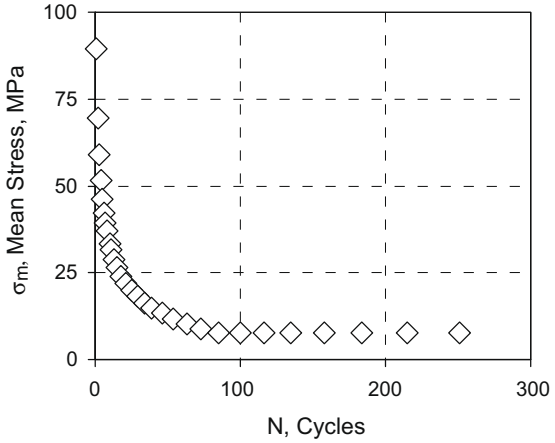

Fig. 1. Mean stress relaxation in an axial test of 7075-T6511 aluminum alloy. The sample was cycled at a strain amplitude of 0.0072 about a mean strain of 0.0108.

In the present study, the Landgraf and nonlinear Maxwell models are used to study mean stress relaxation in three high strength aluminum alloys, 7475-T651, 7075-T6511, and 7249-T76511. The 7075 alloy has been in wide use for more than 50 years in aircraft structural parts and other applications where high strength and light weight are critical. Alloy 7475 is similar but is tailored to achieve improved fracture toughness and resistance to fatigue crack propagation. Alloy 7249 has been developed as a replacement for 7075 to achieve improved resistance to both exfoliation corrosion and stress corrosion cracking. Relaxation curves were obtained by testing under biased strain control and the experimental curves were fitted with the relaxation forms from the models, to obtain models constants and simulate the mean stress relaxation.

2. Mathematical models

The models chosen by the authors to best reproduce mean stress relaxation in the aluminum alloys under investigation were the Landgraf model and a nonlinear Maxwell rheological model. In Landgraf [9], the relaxation behavior is modeled as an exponential with the number of cycle as base,

$$\sigma_{mN} = \sigma_{mi} N^r, \quad \text{where } r = A\left(1 - \frac{\varepsilon_a}{\varepsilon_{aTh}}\right) \quad (\text{a, b}) \tag{1}$$

Here, σ_m is mean stress, with an additional subscript i indicating the initial value, and an additional subscript N the value after N cycles. Also, ε_a is the strain amplitude (half-range), and ε_{aTh} is the threshold value of this quantity. The dependence of the relaxation exponent r on strain amplitude was modeled with the linear expression (b) shown, along with $r = 0$ for $\varepsilon_a \leqslant \varepsilon_{aTh}$. For steels, $A = 0.85$ is employed in Ref. [9], and ε_{aTh} is expressed as a function of hardness. For application to a particular metal that is not a steel, A and ε_{aTh} can be treated as fitting constants.

Various rheological models show time-dependent relaxation when subjected to biased strain and provide a mathematical formulation that seems to lend itself to ease of computation. A Maxwell model with a nonlinear dashpot, represented by Fig. 2, can be adapted to model cyclic mean stress relaxation.

Fig. 2. Spring and nonlinear dashpot model.

In the model there are three constants: a coefficient B and exponent m for the dashpot, which provides creep strain according to $\dot{\varepsilon}_c = B\sigma^m$, and an elastic modulus E for the spring, giving elastic strain $\varepsilon_e = \sigma/E$. When this rheological model is subjected to a step function of constant strain ε, the relaxation response of stress σ with time t is given by

$$\log \frac{\sigma}{\sigma_i} = \frac{1}{1-m} \log \left(tBE(m-1)\sigma_i^{m-1} + 1\right) \qquad (m \neq 1) \tag{2}$$

To adapt this model to cyclic loading, we create an analogy between the constant strain ε and the mean strain for cyclic loading, $\varepsilon_m = \frac{\varepsilon_{max} + \varepsilon_{min}}{2}$. Further, we replace the time t with the number of cycles N, the initial value of stress σ_i with the initial mean stress σ_{mi}, and the stress σ with the mean stress σ_{mN} after N cycles. Thus, we obtain

$$\log \frac{\sigma_{mN}}{\sigma_{mi}} = \frac{1}{1-m} \log \left(NBE(m-1)\sigma_{mi}^{m-1} + 1\right) \qquad (m \neq 1) \tag{3}$$

Some other models were also tried but not found to be viable. For example, an exponential equation of the form $r = ae^{b\varepsilon_a}$ was tried, where a and b are fitting constants. This equation fit data at low strain amplitudes reasonably well, but gave poor results at high strain amplitudes, where mean stress relaxation effects are of greatest significance, and so it was not further pursued.

3. Experimental methods

The 7075-T6511, 7475-T651, and 7249-T76511 aluminum alloys studied are all Al–Zn–Mg–Cu–Cr alloys that are members of the 7000-series of alloys, which are the highest strength class of aluminum alloys. Their strength arises from the combined effect of multiple precipitation hardening reactions involving the various alloying elements. Percentages of the alloying elements vary somewhat and are specified by the initial four digits, such as 7075. In processing, these alloys are first subjected to a solution heat treatment, followed by quenching. Then there is a second stage of heat treatment, called artificial aging, where the strengthening precipitates form at a moderately elevated temperature. The designation T6 indicates this process. Then the additional digits in T651 indicate wrought material that has been stretched by about 2% after solution treatment, to relieve residual stresses, and the additional digits in T6511 indicate the same for extruded material, with some minor straightening after stretching also being permitted in this case [11].

The 7249 aging treatment is carried beyond the point of peak strength, called overaging, as indicated by the T7 designation. The moderate degree of overaging is specified by the next digit as T76, and then the remaining digits in T76511 indicate stress relief by stretching for extruded material, as above. The overaging treatment for this special alloy may involve more than one stage of time and temperature to meet the strength and other property requirements of the specification AMS 4293 [12], with the exact details generally being proprietary to the extrusion supplier.

Unnotched axial test specimens were employed. The long axes of these were parallel to the longitudinal direction of the extrusion for the 7075 and 7249 alloys, and parallel to the rolling direction of the plate for the 7475 alloy. They were tested under strain control using an MTS closed-loop servo-hydraulic testing machine with 50 kN force capacity. This system was equipped with digital computer control and data acquisition software. Preliminary tests were carried out on 7475-T651 alloy, with specimen design as shown in Fig. 3a. The data obtained from these tests were used as a basis for more extensive tests on the other two alloys, for which the specimen geometry of Fig. 3b was employed. Due to the lack of high levels of mean stress at low strain amplitudes in the preliminary tests,

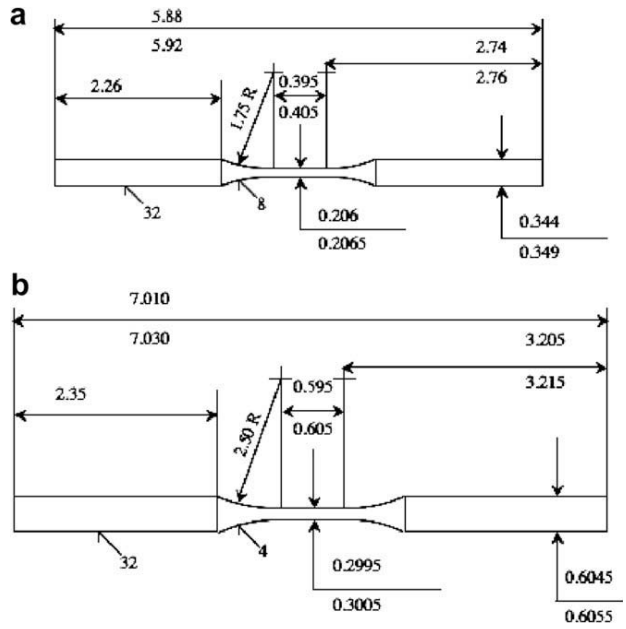

Fig. 3. Test specimen geometries. The dimensions shown in inches.

the strain limits for the tests on the 7075 and 7249 alloys were chosen to cover a wide range of strain amplitudes, 0.2 to 1%, and to obtain mean stresses with values over a wide range, 50 to 450 MPa. Tables 1–3 give the strain amplitudes, ε_a, and mean strains, ε_m, employed, as well as the resulting half life mean stresses, σ_m, and the numbers of cycles to failure, N_f, for the three materials.

Table 1
Test details for 7475-T651 alloy.

Test number	Strain amplitude ε_a	Mean strain ε_m	Mean stress σ_m, MPa	Cycles to failure N_f
1	0.01276	0.00720	−11.43	208
2	0.01075	0.00700	−13.84	369
3	0.01036	0.00361	−10.63	877
4	0.00937	0.00640	−9.04	560
5	0.00878	0.00319	−12.41	423
6	0.00874	0.00901	17.85	306
7	0.00826	0.00973	8.34	928
8	0.00773	−0.00500	−9.89	1660
9	0.00626	0.00350	110.31	2300

Table 2
Test details for 7075-T6511 alloy.

Test number	Specimen number	Strain amplitude ε_a	Mean strain ε_m	Mean stress σ_m, MPa	Cycles to failure N_f
1	75LB-6	0.0095	0.0085	−15.12	439
2	75NLB-1	0.0090	0.009	−11.78	479
3	75LT-5	0.0085	0.0095	−5.18	655
4	75NLB-2	0.0072	0.0108	35.18	2010
5	75RB-5	0.00675	0.01125	70.38	2316
6	75NRB-1	0.0063	0.0117	164.9	2691
7	75LC-3	0.0050	0.013	225.65	4605
8	75LC-2	0.0045	0.0015	83.33	12793
9	75LB-5	0.004	0.014	279.35	9026
10	75LB	0.0030	0.001	60.16	59396
11	75RT-5	0.0025	0.0175	392.80	29054
12	75NLB-3	0.0020	0.015	403.10	37301
13	75RT-6	0.0020	0.006	352.55	36676

Table 3
Test details for 7249-T76511 alloy.

Test number	Specimen number	Strain amplitude ε_a	Mean strain ε_m	Mean stress σ_m, MPa	Cycles to failure N_f
1	49LB	0.00992	0.009003	−17.75	399
2	49LC-3	0.008968	0.008995	−12.48	697
3	49LC-1	0.008486	0.009499	−11.67	781
4	49RB-3	0.007198	0.0108	33.94	1823
5	49LC-4	0.006748	0.011249	61.11	3032
6	49LB-5	0.006298	0.011698	91.80	2851
7	49LT-1	0.004998	0.012999	180.84	6336
8	49NLB-4	0.004659	0.013452	217.96	6731
9	49LT-4	0.003665	0.016982	295.86	87992
10	49NRB-6	0.002363	0.006038	328.52	65000
11	49LC-5	0.002011	0.014875	390.72	41353
12	49MT-C	0.001996	0.006001	328.39	42595

Each test was run with a sinusoidal waveform at a frequency that varied with the plastic strain amplitude involved, ranging from 0.1 Hz at very high strains to 2 Hz where the deformation was primarily elastic. For each test, peak and valley stress–strain data were recorded for all cycles, along with data for complete stress–strain hysteresis loops at logarithmic intervals. The relaxation curves were evaluated at least up to half the life of the specimen. However, in some tests at high strain amplitude with initially tensile mean, the relaxing stress crossed zero and stabilized at a small compressive value. In these cases, the compressive mean stress values were not considered in the analysis.

Following the logic of Topper and coworkers [13,14], initial overstrains were applied to all the specimens prior to the relaxation cycling. This consisted of five completely reversed, strain-controlled cycles at 1.2% strain, followed by 10 additional cycles with peaks and valleys progressively decreasing to zero. This was done to advance the fatigue damage process and the initial transient cyclic hardening, so that the behavior was similar to that during service loading with occasional severe cycles.

When performing the relaxation tests, the response of the servo-hydraulic testing system needed to be carefully tuned. The results of a test before tuning the system are shown in Fig. 4. The strain amplitude and mean strain values gradually shifted and stabilized to the desired values only after 100 cycles. This problem in controlling the strain affected the mean stress response as shown. Stable control of strain during the entire test was possible by carefully optimizing the response settings of the test control system, along with using the automated peak-valley control option of the test system software. For data obtained prior to solving the above test control problem, the entire results of some tests were discarded, and for others, some of the initial data were discarded, especially where the mean strain was not within ± 1% of the stable strain value at half life. For example, only the data collected for $N_f > 100$ cycles were employed for the experimental results reported in Fig. 4.

4. Experimental results and analysis

In this section, we present the preliminary experimental data obtained by testing 7475 aluminum with the Landgraf model fit. Experimental data on 7075 and 7249 alloys collected over a wider range of strain amplitude are then presented. These data were divided in two sets: those for low strain amplitude, and those for high strain amplitude. The two data sets were separately fitted to the Landgraf model and to the previously described nonlinear Maxwell model, as adapted for cyclic relaxation.

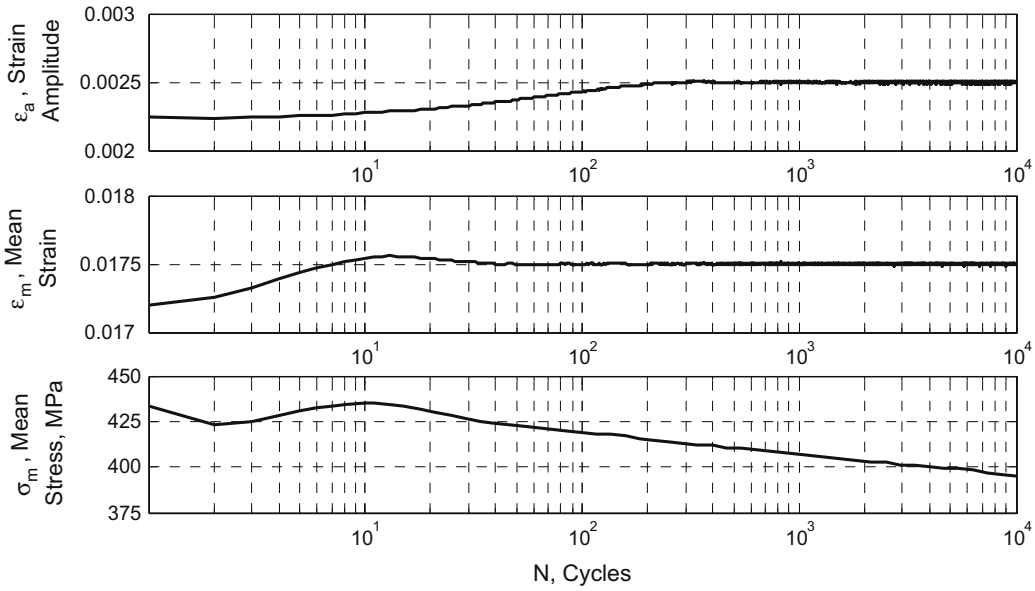

Fig. 4. Variations in the controlled strain amplitude and mean, and the resulting mean stress, during an early test.

4.1. Preliminary results on 7475-T651 aluminum

Recorded peak and valley stress values at various numbers of cycles were used to calculate corresponding mean stresses for 7475 aluminum. The mean stresses were then normalized with respect to the initial ($N = 1$) mean stress in each test to calculate ratios σ_{mN}/σ_{mi} These ratios were then plotted versus the number of cycles on log–log coordinates, as shown in Fig. 5. Note that the results for test no. 5 were not reported for clarity, as they overlap with other curves.

Then, for each test, the data were fitted to the Landgraf model to determine the value of the relaxation exponent r. Specifically, linear regression was employed with Eq. 1(a) in the form

$$\log \frac{\sigma_{mN}}{\sigma_{mi}} = r \log N \tag{4}$$

Eq. (4) corresponds to a straight line with slope r on the log–log plot of Fig. 5. The resulting r values were seen to vary linearly with the strain amplitude as described by Eq. 1(b). See Fig. 6.

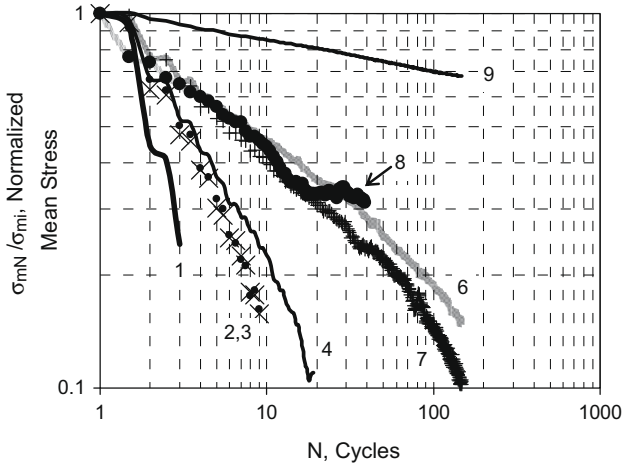

Fig. 5. Normalized mean stress values showing cyclic relaxation in 7475-T651 aluminum. The numbers for the various curves correspond to the *test number* column of Table 1.

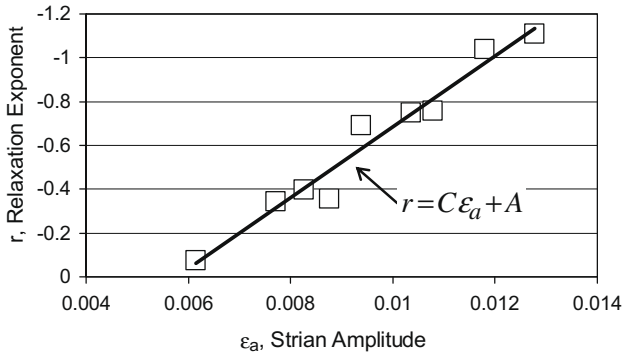

Fig. 6. Relaxation exponent versus strain amplitude data for 7475-T651 aluminum and fitted line.

Further linear regression then gives the equation of the straight line of Fig. 6. The specific form employed is derived from Eq. 1(b) as

$$r = C\varepsilon_a + A, \quad \text{where } C = -\frac{A}{\varepsilon_{aTh}} \tag{5}$$

Values of C and A from the linear fit then allowed ε_{aTh} to be determined, with the results being

$$C = -161.6, \quad A = 0.931, \quad \varepsilon_{aTh} = 0.00576 \tag{6}$$

Also, the regression coefficient for this fit was 96%.

4.2. Landgraf model fitting for 7075-T6511 and 7249-T76511 aluminum

Mathematical manipulation of Landgraf model, Eq. (1), leads to the possibility of performing a multiple linear regression with all of the data points obtained from tests on a particular material. Hence, the trends with both strain amplitude and cycles can be handled in a single fitting procedure. This single fit replaces the stepwise fitting procedure described earlier for the preliminary tests on 7475-T651 alloy.

A first attempt was made to perform such multiple regressions for all of the data for each of the two alloys, but the results were

unsatisfactory, with low correlation values between dependent and independent variables. It was then decided to apply the Fang and Berkovits [10] procedure of partitioning the fitting into two regions. For our data, preliminary stepwise fitting, done in the same manner as described previously for the 7475 alloy, suggested that an appropriate level for separating the two fits is around $\varepsilon_a = 0.6\%$ for both the 7075 and 7249 alloys. This is similar to the $\varepsilon_a = 0.5\%$ value reported in [10], with the value being expected to vary for different materials.

To proceed with multiple regressions in either the high strain or low strain region for a given material, we combine Eqs. 1(a) and (b) and take the logarithm of both sides.

$$\frac{\sigma_{mN}}{\sigma_{mi}} = N^{A(1-\varepsilon_a/\varepsilon_{aTh})}$$
$$\log\left(\frac{\sigma_{mN}}{\sigma_{mi}}\right) = A\log N - \frac{A}{\varepsilon_{aTh}}\varepsilon_a \log N \tag{7}$$

Then a linear, multiple regression is performed by employing the following equation:

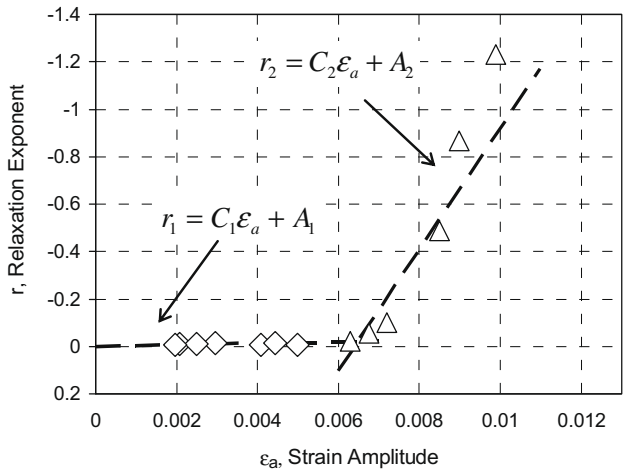

Fig. 7. Relaxation exponent versus strain amplitude data for 7075-T6511 aluminum, with lines from the multiple regression constants also shown.

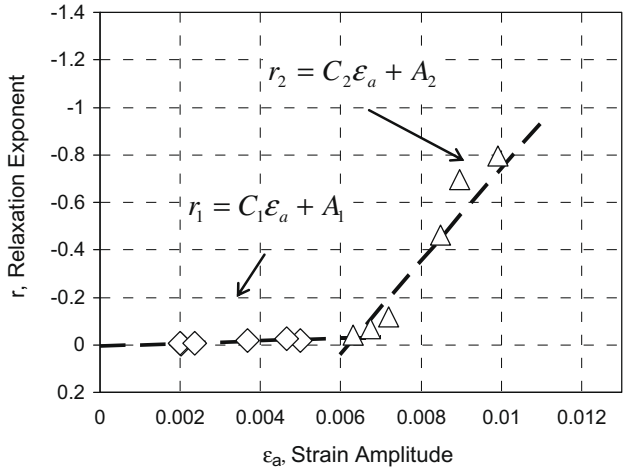

Fig. 8. Relaxation exponent versus strain amplitude data for 7249-T76511 aluminum, with lines from the multiple regression constants also shown.

Table 4
Landgraf model fitting constants for 7075-T6511 and 7249-T76511 aluminum.

Alloy	Range	$m_1 = A$	m_2	ε_{aTh}	Correlation coefficient
7075-T6511	$\varepsilon_a \leqslant 0.648\%$	−0.0006948	−2.92637	−0.0002374	0.8081
7075-T6511	$\varepsilon_a \geqslant 0.648\%$	1.635011	−255.205	0.006407	0.8425
7249-T76511	$\varepsilon_a \leqslant 0.637\%$	0.006347	−5.79367	0.001095	0.8019
7249-T76511	$\varepsilon_a \geqslant 0.637\%$	1.219585	−196.212	0.006216	0.8081

$$y = m_1x_1 + m_2x_2 + b$$
$$\text{where} \quad x_1 = \log N, \quad x_2 = \varepsilon_a \log N, \qquad b = 0 \tag{8}$$

Once the fitting parameters m_1 and m_2 are obtained, the desired constants can be determined,

$$A = m_1, \quad \varepsilon_{aTh} = -\frac{A}{m_2} = -\frac{m_1}{m_2} \tag{9}$$

Partitioning the data for each material into low strain and high strain sets greatly improves its representation by the Landgraf model. The correlation factors are all near or above 0.8, with the fitting constants obtained being listed in Table 4. Plots of the relaxation exponent r of Eq. (1) versus strain amplitude ε_a are shown in Figs. 7 and 8 for the two alloys, with a clear transition in behavior being evident around $\varepsilon_a = 0.6\%$ in each case. The straight lines shown in Figs. 7 and 8 correspond to Eq. (5), but with the constants C and A being obtained from the multiple regression results of Table 4. The strain amplitudes reported under *Range* in Table 4 correspond to transition values that are computed as intersection points of the fitted lines in Figs. 7 and 8.

4.3. Nonlinear maxwell model fitting for 7075-T6511 and 7249-T76511 aluminum

The second model considered as a possible candidate for representing mean stress relaxation, as anticipated in the Introduction, is a Maxwell model with a nonlinear dashpot. The data sets are again divided in two regions depending on the strain amplitude. A stepwise fitting procedure is used, and the normalized curves are fitted to Eq. (3) by using a *Levenberg–Marquardt* fitting procedure [15]. An initial set of mean stress versus cycles fits was done for each test. The values of the exponent m obtained were then averaged in order to run a second set of fits with the average m values for the high and low strain regions for each material. It was observed that for $\varepsilon_a < 0.6\%$, the values of the exponent m were extremely high, in the range $m = 50$ to 100, while for $\varepsilon_a > 0.6\%$, the exponents were lower, in the range 2 to 20.

This second set of fits employed a form that is equivalent to Eq. (3); the fitting routine used a *Levenberg–Marquardt* fitting function with the following form:

$$\log\frac{\sigma_{mN}}{\sigma_{m1}} = A\log(CN+1)$$
$$\text{where} \quad A = \frac{1}{1-m}, \quad C = BES^{m-1}(m-1)\left(\frac{\sigma_{mi}}{S}\right)^{m-1} \tag{10}$$

Since the exponents m were quite high, difficulties in managing the values of B required the additional parameter S to be included, to avoid working with extremely small or extremely large numbers. The value of S was chosen arbitrarily to correspond to a typical σ_m value.

A strong correlation was found between the logarithm of the first multiplying factor of the fitting coefficient C, i.e. the quantity $\log(BES^{m-1})$, and the initial maximum stress, $\sigma_{\max,i} = \sigma_a + \sigma_{mi}$, for the different tests, where σ_a is the stress amplitude; the mathematical expression of the correlations for $\varepsilon_a < 0.6\%$ are shown in

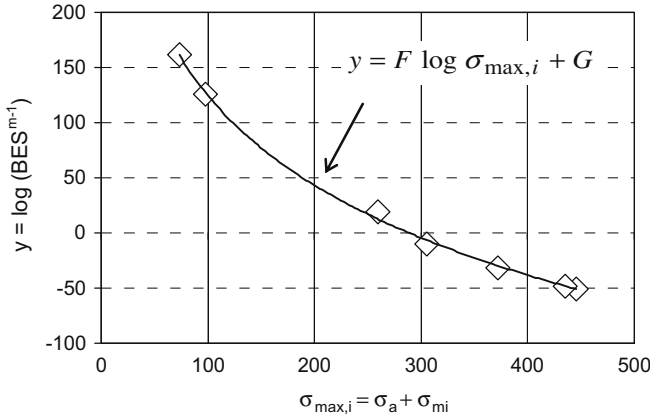

Fig. 9. Correlation of $\log(BES^{m-1})$ with $\sigma_{max,i}$ for 7075-T6511 aluminum.

Table 5
Nonlinear Maxwell model fitting constants for 7075-T6511 and 7249-T76511 aluminum.

Alloy	Range	m	S, MPa	E, GPa	F	G
7075-T6511	$\varepsilon_a \leqslant 0.6\%$	117.28	300	70	−137.58	334.89
7075-T6511	$\varepsilon_a \geqslant 0.6\%$	5.77	300	70	−29.75	59.97
7249-T76511	$\varepsilon_a \leqslant 0.6\%$	50.99	300	70	−270.79	666.22
7249-T76511	$\varepsilon_a \geqslant 0.6\%$	7.20	300	70	−25.63	55.67

Fig. 9. Correlation coefficients for the fits in the low strain region were 0.999 for 7075 and 0.986 for 7249. For $\varepsilon_a > 0.6\%$, similar trends were observed, but with more scatter, and correlation values between 0.7 and 0.8.

The final values of fitting constants are given in Table 5 for both regions for the two alloys. The m values tabulated are of course the average ones employed in the final fitting. Note that the fitting constants F and G provide a convenient way to express the constants so that B values can be calculated for any desired condition of initial stress $\sigma_{max,i} = \sigma_a + \sigma_{mi}$.

4.4. Comparison of models with relaxation behavior

After obtaining model constants from the fitting procedures just described, the ability of the models to correlate with the mean stress versus cycles variation in the same data was examined. For the Landgraf model, a relaxation exponent r was calculated for each strain amplitude value ε_a used in the tests by employing Eq. 1(b) with constants from Eq. (6) or Table 4, as appropriate. For the nonlinear Maxwell model, the average values of m from Table 5 corresponding to the two regions of strain amplitude for each material were employed, and then a value of B was obtained for each test from $\sigma_{max,i}$ by using the mathematical expression of the correlation in Fig. 9 with the appropriate set of additional fitting constants from Table 5.

The model simulations along with the experimental data for the three aluminum alloys are presented in Figs. 10–12. The numbering of the curves in Figs. 10–12 corresponds to the *test numbers* in Tables 1–3.

All the tests for the 7475-T651 alloy have strain amplitudes greater than 0.6%. At the larger amplitudes, the relaxation of initially tensile mean stress crossed zero and stabilizes to a negative (compressive) value. In general, the calculations from the Landgraf model for 7475 aluminum are in reasonable agreement with the experimental data, with a maximum relative error of 15 MPa. Such error is mainly due to the inability of the model to predict relaxation that starts tensile and crosses zero.

For the 7075-T6511 and 7249-T76511 alloys, the amount of relaxation for strain amplitude $\varepsilon_a < 0.6\%$ is modest, with the decay at half life ranging from 15 to 40 MPa relative to the initial value. This contrasts with the magnitude of relaxation for strain amplitude $\varepsilon_a > 0.6\%$, where the decay at half life differs from the initial values by up to 100 MPa. The Landgraf model exhibits generally satisfactory performances both in the low and high strain amplitude regions for both 7075 and 7249 alloys, with maximum errors close to 15 MPa occurring for high strain amplitudes. As for the 7475 alloy, the larger errors are associated with mean stresses that start tensile and crosses zero, which is not predicted by the model.

The predictions obtained via the nonlinear Maxwell rheological model differ considerably in the two strain amplitude regions. For low strain amplitudes, the modeling is quite close to the data, with maximum errors at half life ranging from 5 to 10 MPa. In contrast, for the higher strain amplitudes, the predictions are not as good,

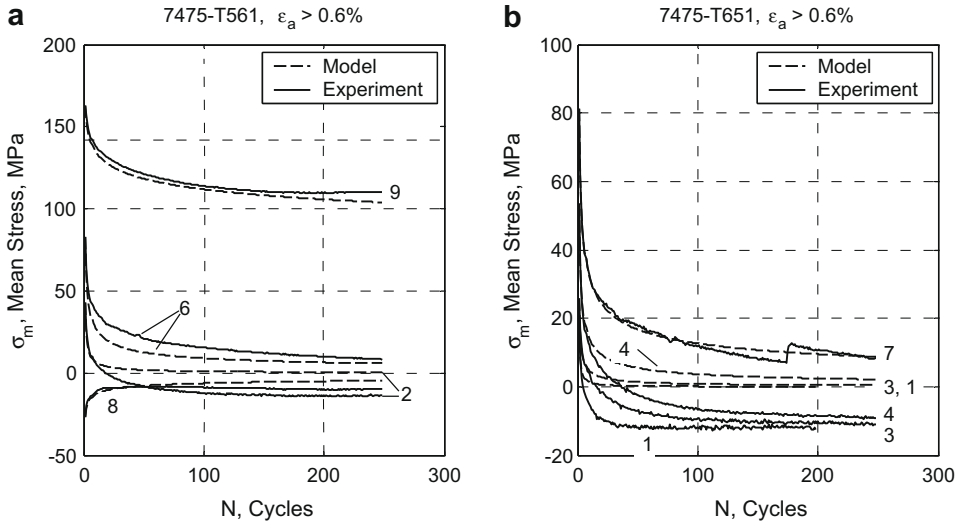

Fig. 10. Simulations and experimental data for the Landgraf model for 7475-T651 Al, with the data separated into two graphs for clarity.

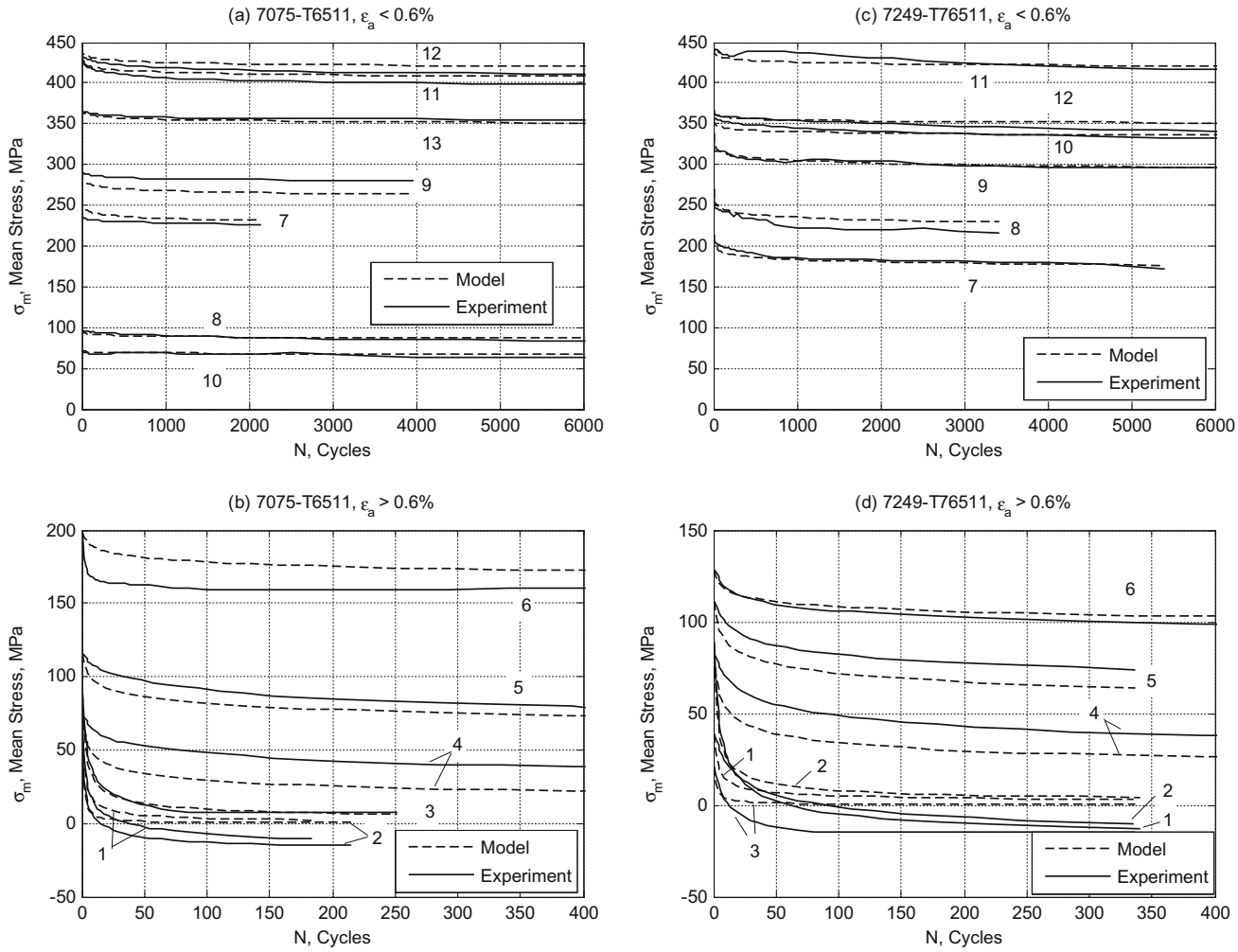

Fig. 11. Simulations and experimental data for the Landgraf model for 7075-T6511 and 7249-T76511 Al.

with maximum errors exceeding 40 MPa, mostly for the lower strain amplitudes that are still in the high strain region.

5. Discussion

The simplicity of the Landgraf model, whether applied with stepwise fitting or with multiple linear regression, is a key factor in the possible choice of this model as an empirical model for relaxation. The dependence of the relaxation exponent r on the strain amplitude ε_a is also intuitive and is in general agreement with other models, such as the one developed by Morrow and Sinclair [7]. But the continued success of this model in the low strain amplitude region, where the plastic strain is negligible or small, is surprising. Hence, the Landgraf model is able to give good predictions for even small amounts of relaxation in cases with minimal plastic deformation.

Although the relaxation formula for the nonlinear Maxwell model is mathematically simple, the high values of the constant m, necessary for accurate fitting, interfered with the manageability of the values of the parameter B, which in turn compromised the final accuracy of the model in comparisons with experimental data for $\varepsilon_a > 0.6\%$. From a computational point of view, the errors for the nonlinear Maxwell model are mainly due to two factors: (1) Since the values of B are obtained from fitting $\log(BES^{m-1})$ against $\sigma_{max,i}$, small differences between the data points and the points on the fitted line will be magnified in modeling. (2) Since the values of m are much greater than unity, every source of error is amplified when the simulation is implemented.

It is significant that, despite these disadvantages, the correlations and predictions obtained for the $\varepsilon_a < 0.6\%$ region were quite good.

The choice of a constant m for the two regions was based on observations of the trends in this value from individual fitting of different tests, and also from previous simulations of relaxation response with varying values of m and B. The dependence of B on the maximum stress was found to provide the strongest correlation with the variables involved in the fitting. It is also notable that differences with strain amplitude within the high or low strain region are not taken into account by a constant value of m.

Also, for the nonlinear Maxwell model, the degree of relaxation in the high strain region is more strongly dependent on the starting point of the curve than is seen in the experimental data. This is likely related to the necessity of using an average m value. Hence, as applied here, this model is not able to incorporate the effects of plastic strain amplitude variation as successfully as the Landgraf model.

As a general consideration, it should be noted that studying mean stress relaxation only in the high strain amplitude region can be inadequate, as in life calculations even a small amount of

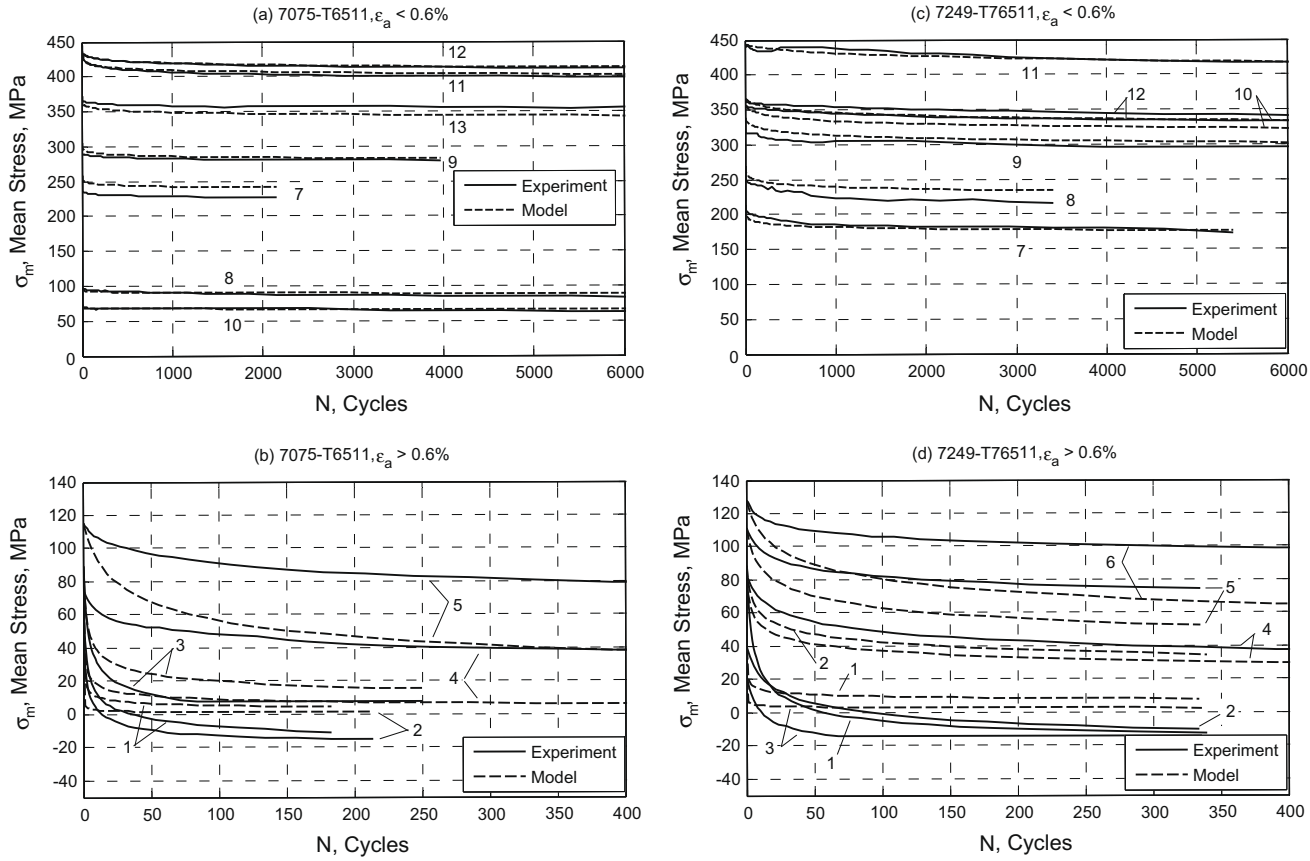

Fig. 12. Simulations and experimental data for the nonlinear Maxwell model for 7075-T6511 and 7249-T76511 Al.

relaxation can be significant. For example, consider test no. 12 on 7075 alloy, which is the test with the highest stress change due to relaxation in the low strain amplitude region. A life estimate with the initial value of mean stress gives a number of cycles to failure that is approximately half that for an estimate using the mean stress at half life.

Further work to extend this study would be useful. First, the relaxation of compressive mean stresses needs to be addressed. One such result is included here for the 7475 alloy, but none for the other two alloys. Compressive mean stresses are of practical interest where compressive surface residual stresses are introduced to extend life, as the benefit will be lost if there is significant relaxation.

A complexity in the behavior that was not addressed in modeling is the crossing of zero during relaxation at high strain levels. However, this effect is of limited practical interest. For initially tensile mean stresses, ignoring it will give a stable value near zero and a conservative (shorter) life estimate than for the relatively small compressive stable value that is observed. For initially compressive mean stresses and high strain amplitudes, as for the single result for the 7475 alloy in Fig. 10, and for one unreported result for 7249 alloy, it appears that the relaxation tends toward a compressive value that is more negative that the model prediction. So again, ignoring the effect is conservative for life estimates.

However, if it is desired to empirically model the zero-crossing behavior, the following modification of Eq. 1(a) is suggested:

$$(\sigma_{mN} + \sigma_b) = (\sigma_{mi} + \sigma_b)N^r \tag{11}$$

Here, σ_b is a bias stress having a positive value. For large values of N, the relaxation stress will approach $\sigma_{mN} = -\sigma_b$. The quantity σ_b should have a nonzero value only for large strain amplitudes, and its value should increase with strain amplitude in a manner consistent with test data.

Noting Eq. 1(b) and Figs. 7 and 8, the ε_{aTh} value for the higher strain fit, which we will denote as ε_{aTh2}, is the ε_a intercept at $r = 0$. Also this quantity has a similar numerical value as the strain amplitude where the fits for the two strain regions intersect. Hence, ε_{aTh2} can be thought of as representing the transition between relaxation behavior involving relatively large plastic strains and behavior involving only quite small plastic strains. With this in mind, it is interesting to place the ε_{aTh2} point on the cyclic stress–

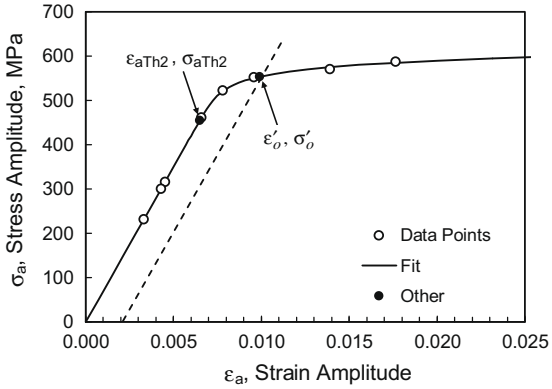

Fig. 13. Cyclic stress–strain curve for 7075-T6511 aluminum with the upper relaxation threshold and the 0.2% offset yield strength shown.

Table 6
Comparison of the upper relaxation threshold and the 0.2% cyclic yield points for the three aluminum alloys.

Alloy	Upper threshold		Cyclic yield		Ratio	
	ε_{aTh2}	σ_{aTh2}, MPa	ε'_o	σ'_o, MPa	$\varepsilon_{aTh2}/\varepsilon'_o$	σ_{aTh2}/σ'_o
7475-T651	0.00576	401.18	0.009615	540.82	0.599	0.742
7075-T6511	0.006407	448.20	0.009904	553.5	0.647	0.810
7249-T76511	0.006216	429.65	0.009695	532.1	0.641	0.808

strain curve of the material, as shown in Fig. 13 for the 7075-T6511 alloy. Note that the ε_{aTh2} point is near the end of the essentially linear portion of the curve, that is, it is near the proportional limit. Hence, the ε_{aTh2} point is somewhat below the 0.2% offset cyclic yield point. A similar trend occurs for the other two alloys, and this behavior is also similar to that observed for steels by Landgraf [9]. Table 6 gives a numerical comparison of the upper threshold point and the 0.2% offset cyclic yield stress and strain for the three aluminum alloys of this study.

6. Conclusions

Regarding the data collected, it is noteworthy that some difficulty was encountered in obtaining high quality mean stress relaxation curves. The measured strains had to be analyzed after each test was complete to avoid fitting data that were affected by imperfect test control. The use of feedback control software and accurate preliminary tests are necessary to assure successful data collection and to reduce the need for test repetition.

Two regions of behavior were observed. As expected, there are large amounts of relaxation at relatively large strain amplitudes. But it was also found that a degree of relaxation can occur even where the plastic strains are very small. The modest stress changes that occurred in the latter situation are nevertheless sufficiently large to be significant from the viewpoint of obtaining accurate life predictions. The two regions of behavior observed suggest that there are two different physical phenomena causing mean stress relaxation in the material when it is subjected to biased strain control, one closely connected with plasticity, and another that can occur with only very small plastic strains.

The current study supports the validity of the Landgraf model as applied to mean stress relaxation. Further, its fitting capability can be successfully extended over a wide range of strain amplitudes by invoking two different regions of behavior.

In addition, it was observed that analogies with static relaxation of rheological models can be postulated, and the equations involved can be adapted and applied to cyclic mean stress relaxation. However, the particular nonlinear Maxwell model studied is not suggested for general use, even though it gave good correlation with some experimental data, especially for $\varepsilon_a < 0.6\%$. This is the case due mainly to difficulties encountered in mathematical manageability and to a low accuracy in the correlations for $\varepsilon_a > 0.6\%$.

Acknowledgements

The authors would like to express their gratitude to the US Naval Air Systems Command, Patuxent River, MD, for financial support, and especially to Nam D. Phan and Trung T. Nguyen of NAVAIR Structures for technical direction. We also thank Pamela F. Bowen of Integrated Systems Solutions, Inc., California, MD, for performing the project administration. A special thanks is addressed to Technical Data Analysis, Inc., Falls Church, VA, for their collaboration in the project work, and in particular to Nagaraja Iyyer and Subhasis Sarkar for their help in planning and supervising the activity. Institutional support was provided by the Engineering Science and Mechanics Department, and by the Materials Science and Engineering Department, Virginia Tech, Blacksburg, VA. We are especially indebted to staff engineer Marshal McCord of the ESM Department, who aided with the laboratory work.

References

[1] Smith KN, Watson P, Topper TH. A stress–strain function for the fatigue of metals. J Mater ASTM 1970;5(4):767–78. December.
[2] Dowling NE. Mean stress effects in stress-life and strain-life fatigue. In: SAE Paper No. 2004-01-2227, Fatigue 2004: second SAE Brasil international conference on fatigue, June 2004, São Paulo, Brasil.
[3] Martin JF, Topper TH, Sinclair GM. Computer based simulation of cyclic stress–strain behavior with applications to fatigue. Mater Res Stand ASTM 1971;11(2):23–9. February.
[4] Wetzel RM. A method of fatigue damage analysis. Ph.D. Thesis, Department of Civil Engineering, University of Waterloo, Ontario, Canada, 1971; see also Technical Report No. SR 71-107, Scientific Research Staff, Ford Motor Co., Dearborn, MI, August 1971.
[5] Socie DF, Morrow J. Review of contemporary approaches to fatigue damage analysis. In: Burke JJ, Weiss V, editors. Risk and failure analysis for improved performance and reliability. New York, NY: Plenum Publishing Corporation; 1980. p. 141–94.
[6] Iyyer N. Fatigue analysis of metallic structures (FAMS). Aerostructures Inc., Arlington, VA, Technical Report 98005, July 1998.
[7] Morrow J, Sinclair GM. Cycle-dependent stress relaxation. In: Symposium on basic mechanisms of fatigue. Philadelphia, PA: American Society for Testing and Materials; 1958. p. 83–109 [ASTM STP 237].
[8] Zhuang WZ, Halford GH. Investigation of residual stress relaxation under cyclic load. Int J Fatigue 2001;23:531–7.
[9] Landgraf RW, Chernenkoff RA. Residual stress effects on fatigue of surface processed steels. In: Champoux RL et al., editors. Analytical and experimental methods for residual stress effects in fatigue. West Conshohocken, PA: American Society for Testing and Materials; 1988. p. 1–12 [ASTM STP 1004].
[10] Fang D, Berkovits A. Mean stress models for low-cycle fatigue of a nickel-base superalloy. Int J Fatigue 1994;16(6):429–37.
[11] Davis JR, editor. Metals handbook: desk edition. Materials Park, OH: ASM International; 1998.
[12] SAE. Aluminum alloy extrusions, 7.9Zn–1.6Cu–2.2Mg–0.16Cr (7249-T76511), solution heat treated, stress-relieved, straightened, and overaged, aerospace material specification. AMS 4293, SAE International, Warrendale, PA; 2008.
[13] Topper TH, Sandor BI. Effects of mean stress and prestrain on fatigue damage summation. Effects of environment and complex load history on fatigue life. American Society for Testing and Materials; 1970 [ASTM STP 462, p. 93–104].
[14] Watson P, Topper TH. The effects of overstrains on the fatigue behavior of five steels. Paper presented at the 1970 Fall Meeting of the Metallurgical Society of AIME, Cleveland, OH, October 1970; see also Watson P. The effect of mean stress and overstrains on the fatigue behavior of structural steels. PhD Dissertation, Department of Civil Engineering, University of Waterloo, Ontario, Canada; 1971.
[15] The Mathworks, Inc. Matlab online reference documentation, <http://www.mathworks.com>.